Variable Dynamic Range Linear-Logarithmic Pixel

Victor TOPORAN

1 STATE OF THE ART

1.1 IMAGE SENSORS

Image sensors detect and measure changes in light intensity, convening the information onto arrays of individual points. They are found in a myriad of devices, from consumer electronics, such as cell phones, to high-end digital cameras, and even scientific equipment such as telescopes and microscopes.

There are two types of digital image sensors - charged-coupled device (CCD), and active-pixel sesnsor (APS). The following will revolve around APSs, as they are most common in consumer devices.

The main working principle behind image sensors is the photoelectric effect, in which photon energy is converted to electrical impulses. This process is performed through photodetectors, such as photodiodes, photogates and pinned diodes. In APS sensors, there are three types of photodiodes: "nwell / psub, n+ / psub and p+ / nwell", as well as two types of photogates: "nMOS transistor gate to drain and pMOS transistor gate to drain". [1]

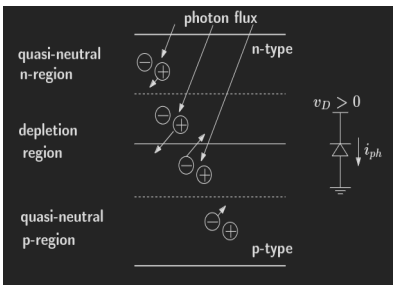

Figure 1.1: Photoelectric effect. [1]

Current through the diode, i_{ph} is generated by three sources of charge [1]:

- electrons in the depletion region - i_{ph}^{sc}
- holes generated in the quasi-neutral n-region - i_{ph}^{p}
- electrons generated in the quasi-neutral p-region - i_{ph}^{n}

1.1.1 Charge gain

The electrons generated in the depletion region are converted directly into current by a strong electric field, while the charge carriers generated in the quasi-neutral regions need to diffuse to the depletion region in order to be collected.

In order to obtain a measurable charge, however, the photodetector needs to be exposed to light for a period denoted as "integration time", t_{int}. After the integration time, the output can be measured as charge, $Q(t_{int})$, or as voltage, $v_0(t_{int})$.

The accumulated charge can be computed with the following [1]:

$$Q(t_{int}) = \frac{1}{q}(i_{ph} + i_{dc})t_{int} \tag{1.1}$$

where q is the electron charge, and i_{dc} is the "dark current", present even when no light hits the photodetector. Because the "well capacity", denoted by Q_{max}, is a known manufacturing constant, the maximum current that can be produced by each pixel can be computed as:

$$i_{ph}^{max} = \frac{qQ_{max}}{t_{int}} - i_{dc} \tag{1.2}$$

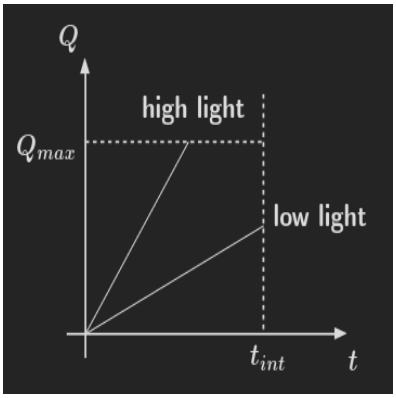

Figure 1.2: Charge accumulation. [1]

As expected, (1.2) showcases that the gained charge is proportional to the integration time, as well as the quantity of light hitting the sensor, with the low light measurement being capped by t_{int} and the high luminosity measurement being capped by Q_{max}.

The photodiode alone is not sufficient to accurately measure the and store the image data, thus several inputs need to be provided alongside the light intensity in order for a pixel to function:

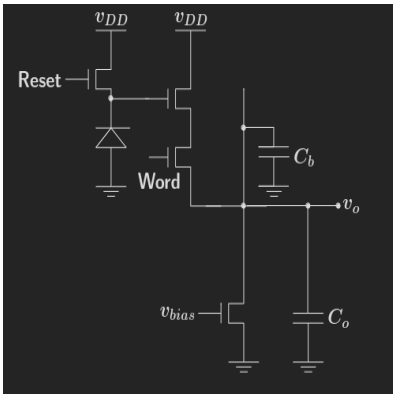

Figure 1.3: APS photodiode pixel. [1]

From (1.3), inputs *Reset* and $Word$ dictate when a pixel value should be set to i_{dc}, respectively when its value should be read. Output v_0 is written to the storage capacitor C_0 whenever the values is requested, and from there it is passed along for further processing.

Individual pixels can only measure the incident light in a small surface area, thus they are grouped into arrays, with common inputs for each row, and common outputs for each column:

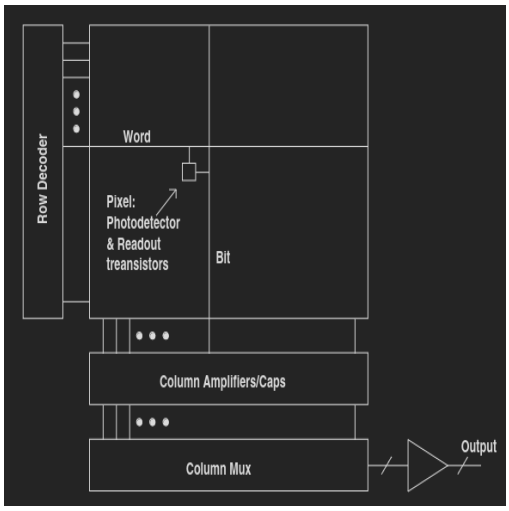

Figure 1.4: Image sensor pixel lattice. [1]

For most APS sensors, in the diagram from (1.4), the row decoder sequential activates each pixel row for recording and output, with the values being sent in parallel to the column capacitors. Due to this behavior, called a "rolling shutter", the environment might change between two consecutive row readouts.

1.1.2 Noise

Due to the dark current, i_{dc}, spots of increased luminosity can be falsely read onto the final image, resulting in noise patterns. Most prevalent in APS sensors is fixed pattern noise (FPN), denoted as such because it is fixed for each sensor. For APSs specifically, FPN is most noticeable across columns, due to amplification, leading to stripes in the final image. [1]

Additionally, fixed pattern noise can be caused by variations in pixel parameters and is quantified as "standard deviation of the spatial variation in pixel outputs under uniform illumination", with reported experimental deviations of $< 1\%$ to $> 4\%$.

1.2 DYNAMIC RANGE

Dynamic Range (DR) represents the ratio between the highest and lowest recorded pixel values. Measured in dB, it can be represented by

$$DR = 20log_{10}(\frac{i_{max}}{i_{min}}) \tag{1.3}$$

where i_{max} and i_{min} represent the maximum, and minimum intensities.

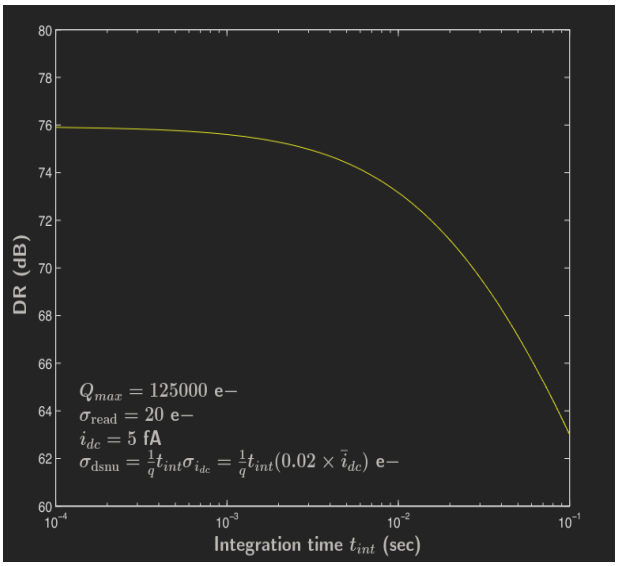

Figure 1.5: Dynamic range versus integration time. [1]

With the value of each pixel increasing linearly with the integration time t_{int}, it follows that the DR will decrease as all pixels approach saturation, as seen in (1.5). [1]

Due to the aforementioned limitation, the dynamic range of most consumer grade sensors is severely limited, when compared to the scenes meant for capture.

Dynamic range varies for different capture devices with the human eye averaging around $90dB$, CCDs between $66dB$ and $> 78dB$, and consumer APSs at around $54dB$. [1]

As a consequence, there is a constant research towards increasing the dynamic range of CMOS sensors, with a constant balance between increasing the maximum intensity, decreasing the dark current and managing timing and storage constraints. Each of those parameters can be a source of noise, another facet that needs to be accounted for when researching image sensor improvements.

1.3 METHODS OF INCREASING DYNAMIC RANGE

1.3.1 Multi-Sampling

Multi-sampling refers to the sequential capture of two identical frames, with different integration times, in order to capture both high and low light regions. In the particular case of dual sampling, the same row is read twice, with a reset between each read. The resulting images are passed along to a designated processing unit, where they can be combined linearly (through bit concatenation) or non-linearly (through addition). [2]

Another technique researched is that of "Predictive Multiple Sampling", in which a selected interval is used as a reference point for a set of shorter integration times, all having a common end point. Out of this set, an optimal interval is chosen based on recorded pixel values "while a pixel saturation predictive decision is used to overlap the integration intervals within the given integration time such that only one frame using the optimal integration interval for each pixel is produced". [3]

Experimental results for both methods showcase a possible dynamic range of $70 - 108dB$, at the expense of increased noise distortion. [2], [3]

1.3.2 Time to Saturation

This method relies on different integration times for each pixel, requiring the addition of signal processing components directly into the sensor circuitry. The process can vary, depending on weather the image is to be used by itself or in a video stream.

For single images, the intensity i_{ph} can be computed as

$$i_{ph} = \begin{cases} \frac{qQ_{max}}{t_{sat}}, & i_{ph} > \frac{qQ_{max}}{t_{int}} \\ i_{ph}, & i_{ph} < \frac{qQ_{max}}{t_{int}} \end{cases} \tag{1.4}$$

where t_{sat} is the saturation time of the photodetector. In this case, the additions to the circuit conssit of a comparator, and a capacitor used to store the duration. Both the input from the diode, as well as the time-stamp, are passed to an ADC, with the computation being done in the digital domain. [1]

Another implementation is based on a sequence of frames, with the previous readout influencing the one currently occurring. In this case, after every integration interval, a check for saturation or "motion" is performed on each pixel. This is done through a comparison between the current

pixel charge and the previous report, based on a given threshold value th_m. If the difference between the two values exceeds the threshold, both values are sent to the controlling circuit. At the same time, saturation is also checked for, using a different threshold, th_s, in which case the voltages are again sent to the main circuit, and the photodetector is reset. If neither condition is met, no output is provided, and the diode continues to integrate. [4]

This method is able to achieve a dynamic range of 56dB, but it is costly both in terms of circuit complexity, as well as power consumption. [1], [4]

1.3.3 Linear-Logarithmic Response

The approach used in this project, this method relies on changing between a linear response to the charge on the photodiode, to a logarithmic one, based on a given threshold value. Due to the different characteristic curves, an increased dynamic range is achieved by having an increased range of resulting values, when compared to each individual response.

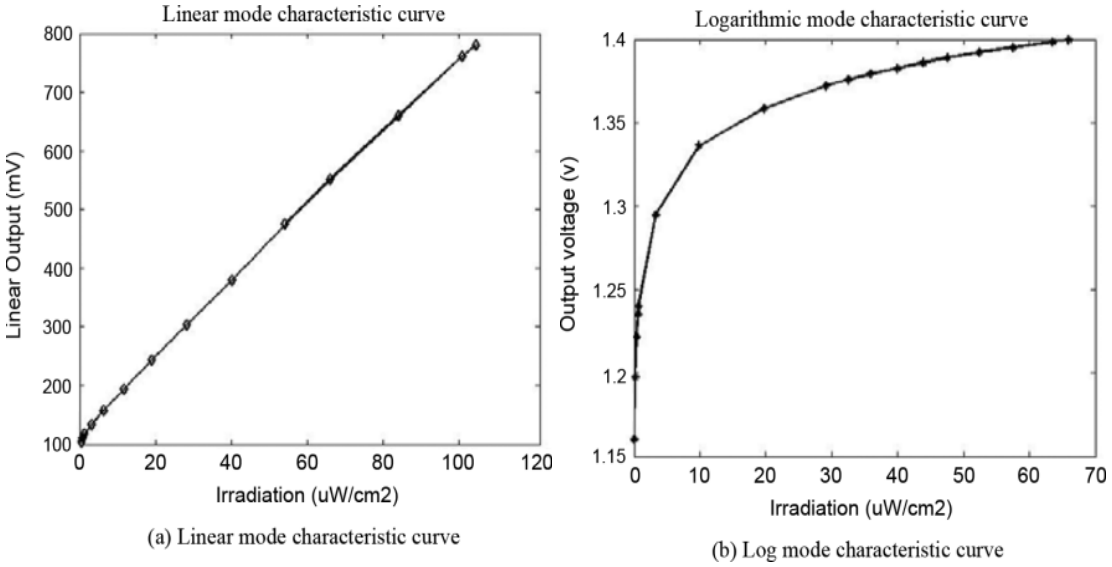

Figure 1.6: Linear and logarithmic characteristic curves. [5]

As showcased in (1.6), for low light conditions the linear response provides a greater range of values for low light intensity, with the output voltage spiking as luminosity increases. In contrast, the logarithmic response provides little accuracy for low light, with the output values clumping as the intensity spikes.

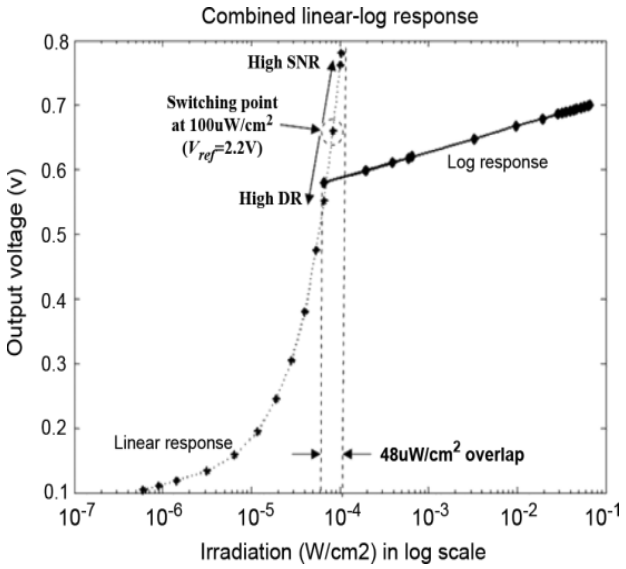

Figure 1.7: Combined characteristic curve. [5]

Because of the exponential nature of the charge gain, combining the two responses generates a better coverage of the entire luminosity spectrum, as shown in (1.7).

2 PAPER DESCRIPTION

For this project, "Combined Linear-Logarithmic CMOS Image Sensor with FPN Calibration" was chosen, because it not only presents improvements upon previous work, but it also provides a stepping stone for adaptive thresholding of linear-logarithmic response image sensors. On top of this, it also provides a solution to the fixed pattern nose present in such systems.

The paper presents a pixel structure that is able to automatically switch between linear and logarithmic response, based on a threshold voltage. It also showcases an FPN mitigation technique, through the use of a two-step charge transfer from the photodiode. [6]

2.1 MOTIVATION

The paper aims to bring the dynamic range of conventional image sensors, $60 - 80dB$, closer to the DR of naturally occurring scenarios, able to surpass $180dB$. Compared to multi-sampling and well adjustment, this method induces high FPN, due to the threshold gap between the linear and logarithmic responses, which would need to be corrected by other processing steps. In order to reduce the overall cost, both in terms of image processing steps, as well as pixel structure complexity, the paper introduces a charge transfer process in two steps. [6]

2.2 IMPLEMENTATION

Pixel architecture is based on "conventional 4T pixel with a charge compensation phototransistor", with the P+ layer connected to an external voltage, used for thresholding between linear and logarithmic modes.

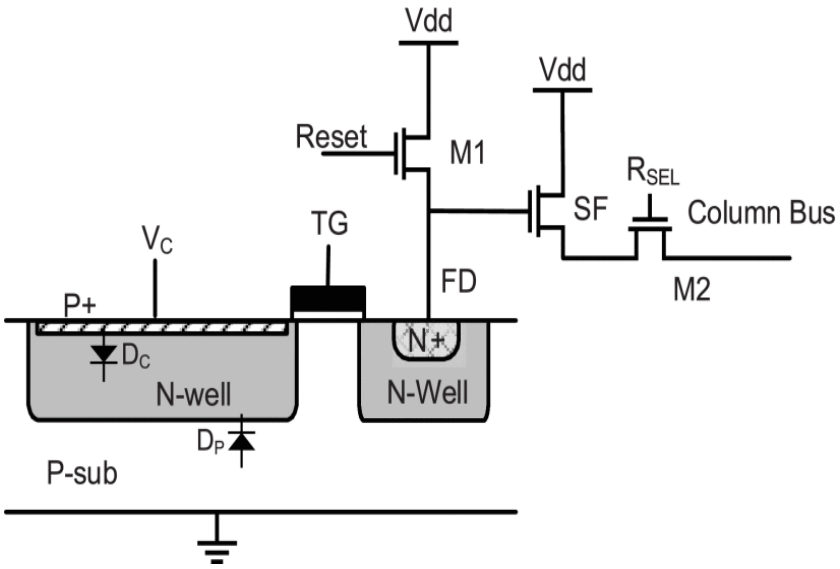

Figure 2.1: Pixel schematic. [6]

The schematic provided in (2.1) represents the charge compensation mechanism, centered around photodiodes D_c and D_p. The anode of diode D_c connected to the variable voltage source V_C, called the compensation voltage. The cathode of D_c is connected to the cathode of diode D_p. At the beginning of the integration time, the potential of output V_p is higher than V_C, and D_c is reverse biased to D_p. As illumination increases, the generated charge causes the potential of V_p to drop under V_C, and D_c to become forward biased to D_p. In this case, photodiode D_c provides the compensation current, in addition to D_p. [7]

From the aforementioned relations, one of two distinct readouts are provided by the pixel for a given intensity. In the first case, at low illumination, or short integration time, charges are stored in the depletion layer and "transmitted to the node capacitor C FD when TG is turned on", and the output is linear:

$$V_{out-lin} = V_{DD} - \frac{t_{int} I_P}{C_{FD}} \tag{2.1}$$

At high intensity, or for long integration time, the current provided by the photodiode D_p is compensated by the current from D_c:

$$I_P = I_S \exp\left(\frac{V_c - V_{out}}{V_T} - 1\right) \tag{2.2}$$

with I_S denoting the saturation current provided by D_c, and V_T denoting the thermal voltage. Thus, the output is resolved logarithmically:

$$V_{out-log} = V_C - V_T \ln \frac{I_P}{I_S} \tag{2.3}$$

The dual response allows for good response in low light conditions, using linear mode, as well as avoiding "premature pixel saturation", using the logarithmic mode. [6]

For "conventional linear-logarithmic pixels", the output signal is permeated in a single transfer, leading to increased fixed pattern noise, that has to be corrected for in the digital domain. To mitigate the FPN without the use of digital signal processing resources, a two-step charge transfer process is used, based on the TG gate. [8]

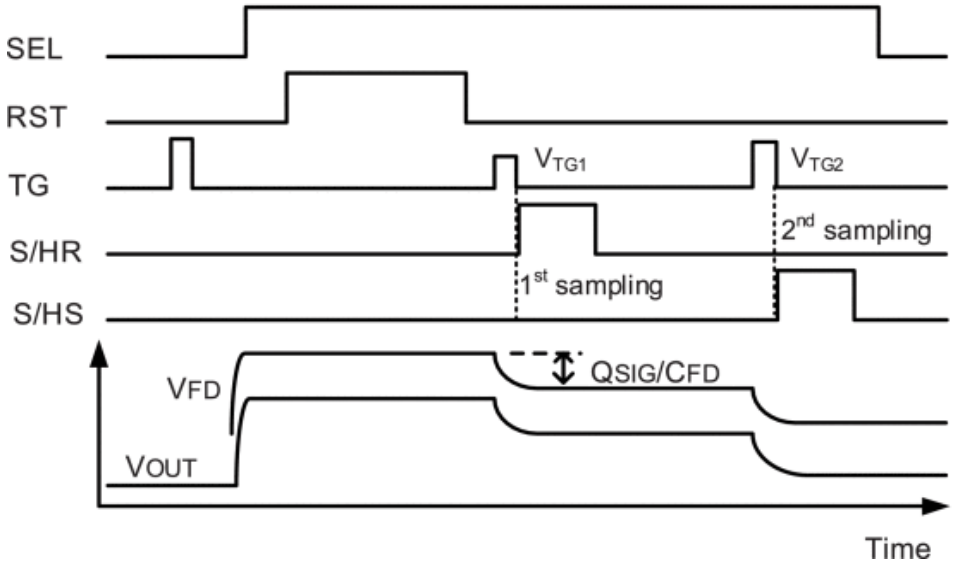

Figure 2.2: Timing diagram for two-step charge transfer. [6]

As mentioned previously, at high luminosity or integration time, D_c acts as a current source, and compensates the charges generated by D_p, charges that "increase logarithmically over the barrier under the TG". The first read step happens under a lower voltage, V_{TG1}, on a partial signal value. After it is read out, a second transfer step occurs, unger V_{TG2}. Finally, one of the desired values is picked, based on the desired FPN, removing the requirement for further processing. [6]

2.3 RESULTS

The design was tested using a prototype sensor with a resolution of $160x200$ pixels, "fabricated in $0.18\mu m$ standard CMOS process IP6M technology. Voltage V_C was tweaked across the tests, in order to obtain the optimal threshold value for maximum dynamic range. [6]

Table 1: Dynamic range and switching points, based on V_C

V_C (V)	0	0.5	1	1.5	2
Switching point $(mW/cm2)$	0.6	0.54	0.4	0.25	0.12
Dynamic range (dB)	122	143	159	169	165

As seen in (1), the maximum dynamic range is obtained for a threshold of $1.5V$, peaking at $169dB$. This was also the case for which the output was graphed, however, the original proposal for the linear-logarithmic pixel provides more relevant data:

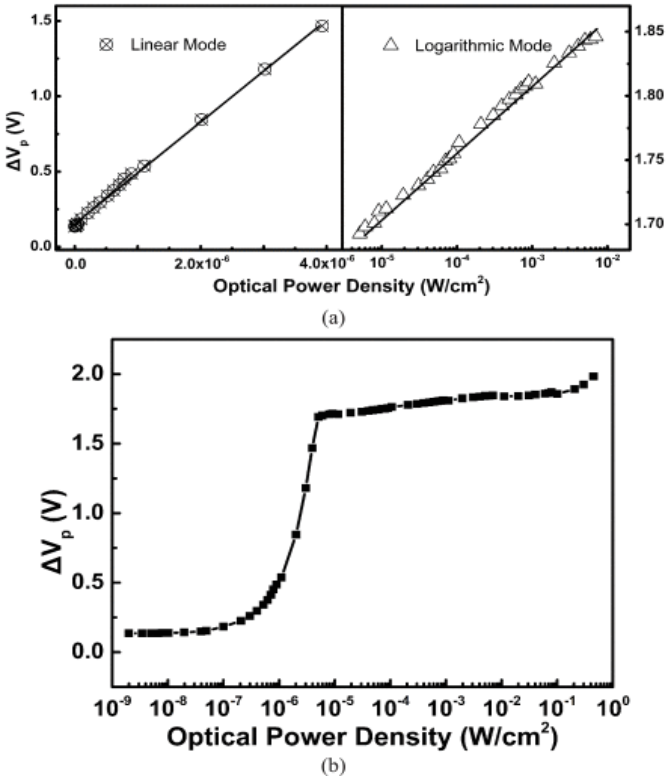

Figure 2.3: Linear-Logarithmic response scaled. [7]

(2.3) provides a more detailed explanation for the linear and logarithmic behavior, with the difference between the measurements being the scale difference of the luminosity. Notably, the logarithmic response provides the same value range, when the increase in light intensity is exponential.

REFERENCES

[1] A. E. Gamal. "EE392B: Introduction to image sensors and digital cameras." (2015), [Online]. Available: https://isl.stanford.edu/~abbas/aeglect392b.php.

[2] O. Yadid-Pecht and E. Fossum, "Wide intrascene dynamic range cmos aps using dual sampling," *IEEE Transactions on Electron Devices*, vol. 44, no. 10, pp. 1721–1723, 1997. DOI: 10.1109/16.628828.

[3] P. Acosta-Serafini, I. Masaki, and C. Sodini, "Predictive multiple sampling algorithm with overlapping integration intervals for linear wide dynamic range integrating image sensors," *IEEE Transactions on Intelligent Transportation Systems*, vol. 5, no. 1, pp. 33–41, 2004. DOI: 10.1109/TITS.2004.825089.

[4] T. Hamamoto and K. Aizawa, "A computational image sensor with adaptive pixel-based integration time," *IEEE Journal of Solid-State Circuits*, vol. 36, no. 4, pp. 580–585, 2001. DOI: 10.1109/4.913735.

[5] J. Guo and S. Sonkusale, "A high dynamic range cmos image sensor for scientific imaging applications," *IEEE Sensors Journal*, vol. 9, no. 10, pp. 1209–1218, 2009. DOI: 10.1109/JSEN.2009.2029814.

[6] S. Cui, Y. Mu, N. Ding, J. Jiang, and Y. Chang, "Combined linear-logarithmic cmos image sensor with fpn calibration," in *2018 IEEE International Conference on Integrated Circuits, Technologies and Applications (ICTA)*, 2018, pp. 128–129. DOI: 10.1109/CICTA.2018.8706097.

[7] S. Cui, Z. Li, C. Wang, X. Yang, X. Wang, and Y. Chang, "A charge compensation phototransistor for high-dynamic-range cmos image sensors," *IEEE Transactions on Electron Devices*, vol. 65, no. 7, pp. 2932–2938, 2018. DOI: 10.1109/TED.2018.2837140.

[8] J. Lee, I. Baek, D. Yang, and K. Yang, "On-chip fpn calibration for a linear-logarithmic aps using two-step charge transfer," *IEEE Transactions on Electron Devices*, vol. 60, no. 6, pp. 1989–1994, 2013. DOI: 10.1109/TED.2013.2259236.